Available online at www.rilem.net

Materials and Structures **38** (December 2005) 865-873

Natural frequency evaluation of a cracked RC beam with or without composite strengthening for a damage assessment

M. Massenzio, E. Jacquelin and P.A. Ovigne
L2MS UCBL Lyon I, France

Received: 17 December 2004; accepted: 11 January 2005

ABSTRACT

This study focuses on the natural frequency determination of a cracked reinforced concrete beam. In a first step, the influence of the steel rebars inside the concrete beam is studied and an analytical approach is proposed for the modelling of a cracked beam with composite strengthening. An experimental validation is carried out on small-scale reinforced concrete beam. In a second step, a prevision of the cracking pattern is implemented in the modelling so as to predict the natural frequencies of a beam as a function of the maximal moment which was applied to the beam. This is experimentally validated with small-scale models and it is shown how that may be used to assess the damage of a beam.

RÉSUMÉ

Cette étude s'intéresse à la détermination des fréquences propres d'une poutre en béton armé, renforcée ou non par un matériau composite. Dans un premier temps, l'influence des armatures en acier est étudiée et une modélisation d'une poutre BA renforcée par composite est proposée. Une validation expérimentale est effectuée sur des modèles réduits. Cette modélisation, associée à une prédiction réglementaire du schéma de fissuration, est utilisée pour prédire le moment maximal qui a été appliqué au système. Cette prédiction est basée sur la détermination du décalage des fréquences propres : en effet, ce décalage est caractéristique de l'endommagement de la structure.

1. INTRODUCTION

Civil engineers often encounter structural problems due to physio-chemical damages (alkali-reaction, carbonation) and mechanical damages due to overloads or accidental loadings [4]: so, it is of the utmost importance to be able to assess the structure damage, so as to strengthen the structures if it is necessary. For the past two decades, external strengthening involving composite material strengthening has appeared as an innovative technique to solve these problems. The wide range of composite materials and their high specific mechanical properties make them very attractive for this purpose [1, 2, 9, 13].

The measurement and the prediction of the modal scheme components (natural frequencies and mode shapes) of a structural member can be used for its damage assessment and its long time survey. So, the modal analysis can be considered as a tool for a structural fault diagnosis and then, can be useful to plan reinforcement. Although numerous studies have already been carried out on the static behaviour of structures with composite reinforcement, the influence of the composite on the dynamic characteristics of reinforced structures had yet to be explored. That is why an analytical model of a cracked beam with composite strengthening has been developed in [10]. This model has enabled the study of the force transfer in the vicinity of cracks to quantify the influence of the shearing of the resin joint on the natural frequencies of a cracked beam with composite strengthening [11].

Vibration of cracked reinforced concrete beams was subject of various studies in the past decades [7, 8, 17] and cracking was considered as a reduction of the inertia: an equivalent inertia I_{eq} or a bending stiffness EI_{eq} was derived. Such an approach does not take into account the degrees of freedom associated with the lips of the cracks. As a consequence, a crack-bridging effect due to the tension reinforcement or the composite external strengthening cannot be taken into account. As a consequence, a specific analytical model integrating the local effects of the lips has been developed in [10]. The present paper is based on the improvement of this model. This latter is used as an analytical tool in order to see in what extends the rebars influence the natural frequencies of a cracked beam. This model is eventually used as a prediction tool of the natural frequencies of a beam experiencing cracking caused by a static loading.

doi:10.1617/14235

First, the experimental and analytical means are presented. Afterwards, a modelling of a cracked reinforced concrete beam with a composite strengthening is proposed and is experimentally validated on a small-scale model; a prediction of the cracking pattern as a function of a static loading is then implemented as an input of the model so as to provide a prediction of the evolution of the frequencies. This prediction is compared to experiments carried out on small-scale models.

2. EXPERIMENTAL

2.1 Small scale model of RC beam

The specimens used for this study are small-scale models of a reference beam (scale 1:1), which has been designed according the French code BAEL [3]. This beam has to resist a four-point 50 kN service load. Furthermore, it is designed in order to fail by tension (yielding of the tension reinforcement). Such a failure mode justifies its external strengthening by the mean of a composite plate bonded on the tensile face. This reference beam was tested in the laboratory in order to carry out static tests for the study of composite strengthening [16].

Whereas the size of this beam is well adapted to static experimental means to our own Fig. 1, the measurement of the natural frequencies according to the experimental procedure used in this study and described below, is further complicated:

- static loading-unloading cycles coupled with the handling to set the samples in a free-free boundary conditions,
- dynamic characterization of the beam: the equipment required to test the actual beam is more difficult to use and more expensive.

Then, for practical reasons, small-scale models of the reference beam are used Fig. 2. A set of scale factors is derived from a dimensional analysis of the various terms encountered in the study of both static and dynamic bending of RC beams. The scale factors are used to experimental data conversions from one scale to another.

Reference beam: 1:1 scale

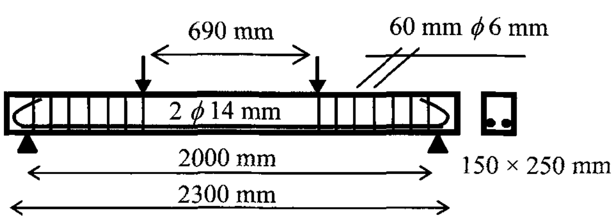

Fig. 1 - Dimensions of the reference beam.

1:3 scale model

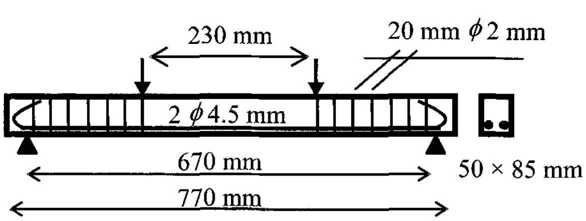

Fig. 2 - Dimensions of the small-scale model.

2.2 Composite external strengthening

The composite material used to strengthen the beam is made of two layers of a unidirectional carbon fiber wrap impregnated with epoxy resin (G_{resin}= 1200 MPa). The carbon wrap characteristics are the following: toughness 3400 MPa, Young modulus 230000 MPa, weight: 200 g/m^2. The longitudinal Young modulus of the resulting composite is E_{compo}= 70000 MPa. The composite strengthening is bonded on the tensile face of the beam.

2.3 Static measurements

First, the static behaviour of the small-scale model is checked within the elastic field. A four point bending test is carried out on the reference beam [16] and on the small-scale models. Strain gauges are placed on the tension rebars and on the compressed fiber at the midspan section. At this section, the strain for various depths is measured edgewise so as to determine the curvature and the neutral axis position. The experimental data obtained from small-scale models (1:3) were converted to 1:1 scale and compared to the reference ones.

Regarding the curvature and the neutral axis position, the results from the small-scale model satisfactorily agree with the results form the full-scale model: a 10% concordance is observed which is commonly encountered when working with small-scale RC models. These two parameters are representative of the static equilibrium resulting from the rebars tension and the concrete compression. Hence, this test provides the assurance that the static phenomena encountered in the reference case are correctly represented at 1:3 scale.

2.4 Dynamic measurements

The natural frequencies of the beam are measured with free-free boundary conditions: that consists in hanging the beam on elastic bonds whose stiffness is much less than the value of the beam stiffness. Then a modal analysis is performed by analyzing the transfer function between different excitation and measuring points. An impact hammer (Bruel and Kjær 8202 with a force transducer B&K 8200) is used for supplying a large frequency bandwidth impulse (0-10 kHz) on the beam (several positions). The excitation is perpendicular to the beam. An accelerometer (Metravib 103M) fixed at several positions on the beam, is used to record its response. A Siglab analyzer that allows the frequency content to be explored, analyzes the excitation and the response, and provides the magnitude and phase of the transfer function.

So, the experiments performed in this article are a succession of static increasing loads and of dynamic measurements: at each step, first, the beam is statically loaded up to a given level, and then it is unloaded and hung to carry out the dynamic experiments.

3. BACKGROUND

3.1 Analytical model of a cracked beam with external strengthening

An analytical model of a homogeneous beam which features open cracks is based on the assembly of beam elements k, connected by elastic hinges, Fig. 3 [6, 10].

The crack between the beam elements k-1 and k is described by the two vectors q^{k-1}_{right} and q^{k}_{left}; both of them include two displacements (the vertical translation v and the rotation θ) and two efforts (the shear force P and the bending moment M):

$$q^{k}_{right} = \begin{bmatrix} v \\ \theta \\ P \\ M \end{bmatrix}^{k-1}_{right} \qquad q^{k}_{left} = \begin{bmatrix} v \\ \theta \\ P \\ M \end{bmatrix}^{k}_{left} \tag{1}$$

The vectors q^{k-1}_{right} and q^{k}_{left} are not independent: they are connected by the transfer matrix of the crack:

$$\begin{bmatrix} v \\ \theta \\ P \\ M \end{bmatrix}^{k-1}_{right} = \begin{bmatrix} 1 & 0 & 0 & 0 \\ 0 & 1 & 0 & C_{22} \\ 0 & 0 & -1 & 0 \\ 0 & 0 & 0 & -1 \end{bmatrix}^{k} \begin{bmatrix} v \\ \theta \\ P \\ M \end{bmatrix}^{k}_{left} \tag{2}$$

The stiffness $k^{\theta}_{crack} = 1/C_{22}$ of the hinges is derived according to the stress concentration around the crack tips [6, 12].

This previous modelling has been improved to take into account an external strengthening [10]. It appeared that the crack-bridging force transfer mechanism (due to the shearing of the resin joint between the beam and the composite) is quite influent on the stiffness of the strengthening and then on the natural frequencies. It is shown that the composite strengthening is only active in the crack vicinity along an active length quoted L_{compo}. An analytical approach, based on a modal extension of Täljsten's model [14, 15], makes possible the determination of L_{compo} by determining shear stress mode shapes of the resin joint [11]. So, to account for the composite strengthening, the stiffness k^{θ}_{repair} must be added to the hinge stiffness:

$$k^{\theta}_{repair} = h^{2} \frac{E_{compo}\, S_{compo}}{L_{compo}} \tag{3}$$

where h is the beam height, and E_{compo}, S_{compo}, L_{compo} are respectively the Young's modulus, the area, the active length of the composite strengthening.

Thus, the cracked section with external strengthening is modelled by an elastic hinge whose stiffness k^{θ}_{hinge} is given by:

$$k^{\theta}_{hinge} = k^{\theta}_{crack} + k^{\theta}_{repair} \tag{4}$$

Then, the flexibility C_{22} in the transfer matrix must be replaced by the following flexibility:

$$\overline{C}_{22} = \frac{1}{k^{\theta}_{hinge}} \tag{5}$$

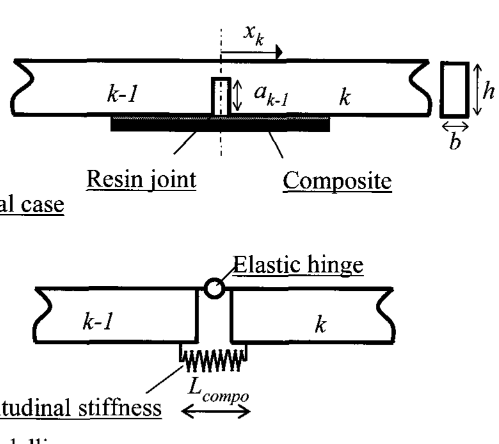

Fig. 3 - External strengthening of a cracked section.

3.2 Determination of the natural modes

The natural vibration modes of the entire beam are calculated from the assembly of all the beam elements, the strengthened crack modelling. The beam elements are described by the Timoshenko theory where the transverse displacement $v(x,t)$ and the section rotation $\theta(x,t)$ are used. To find the natural modes, $v(x,t)$ and $\theta(x,t)$ are supposed to be a standing wave: the space and time variables are separated. This provides the following expressions:

$$v(x,t) = v(x)e^{i\omega t} \tag{6}$$

$$\theta(x,t) = \theta(x)e^{i\omega t} \tag{7}$$

where ω is a natural angular frequency.

According to the governing equations of the beam element, the displacement magnitudes can be written as:

$$v(x) = \sum_{j=1}^{4} A^{k}_{j} e^{p_j x} \tag{8}$$

$$\theta(x) = \sum_{j=1}^{4} \left(p_j + \frac{m\omega^2}{p_j k A_{beam} G_{beam}} \right) A^{k}_{j} e^{p_j x} \tag{9}$$

where p_j (j=1 to 4) are the four wave numbers derived from the characteristic polynomial associated with the fourth degree equation of motion of a Timoshenko beam (mass per unit length m, cross section A_{beam}, inertia I, Young's modulus E, shear modulus G_{beam}, shear factor k); A_j^k are constants that can be determined considering the boundary conditions.

The shear force P and bending moment M magnitudes can then be expressed as:

$$P(x) = \sum_{j=1}^{4} \frac{m\omega^2}{p_j} A_j^k e^{p_j x} \qquad (10)$$

$$M(x) = \sum_{j=1}^{4} EI\left(p_j^2 + \frac{m\omega^2}{kA_{beam}G_{beam}}\right) A_j^k e^{p_j x} \qquad (11)$$

This formulation is presented in further details and has been confronted to a finite element simulation in [10]. Moreover, this approach has been confronted to experiments in the case of steel notched beams with a composite external strengthening [11].

4. MODELLING OF A CRACKED RC BEAM WITH COMPOSITE STRENGTHENING

The models previously described have been validated on systems with 'clean' and controlled cracks. Our aim is now to extend it to an actual cracked reinforced-concrete beam; so the crack pattern includes swaying and non-vertical cracks which are bridged by the steels rebars.

4.1 Steel rebars crack bridging: experimental approach and modelling

The natural frequencies of a small-scale model are measured for the intact configuration and for the cracked one (the beam is designed according to the French code BAEL, to resist a 5.6 kN load; it is statically loaded up to 10 kN then unloaded and finally placed in free-free boundary conditions to be dynamically tested). The experimental results are then compared to the analytical ones (Timoshenko homogeneous beam with E_{beam}= 3.3 10^{10} Pa and ρ_{beam}= 2350 kg/m^3) in order to see in what extend the steel rebars influence the frequencies of a cracked RC beam (Tables 1 and 2).

The results show that the steel rebars have no significant influence on the natural frequencies of an intact beam. Their mass and bending stiffness are not high enough to significantly modify the natural frequencies. Then, an intact RC beam can be modelled as a homogeneous concrete beam. On the contrary, when the beam features cracks, the steel rebars influence is significant and the modelling must take them into account in order to ensure good concordance with experiments (Table 2). The rebars are placed in order to reduce crack opening. As a consequence, they play the role of crack bridging elements inside the beam. Then, they are modelled in a similar manner as described in (§ 3.1) for the composite. The effect of the steel rebars strengthening is superimposed to the one of the composite (Fig. 4).

Yet, whereas the active length of the composite can be evaluated from shear stress mode shapes inside the resin joint

Table 1 - Natural frequencies (Hz) of an intact RC beam. Experience and modelling

Mode number	Experiment (Hz)	Modelling (Hz)	Difference (%)
1	530	530	0.0
2	1340	1370	2.2
3	2460	2470	0.4
4	3750	3730	0.5
5	5100	4820	5.5

Table 2 - Natural frequencies (Hz) of a cracked RC beam (10 kN) without composite

Mode number	Experiment (Hz)	Model with rebars (Hz)	Model without rebars (Hz)
1	407	415	107
2	1070	1129	345
3	2083	2174	774
4	3079	3233	1187
5	4245	4593	2120

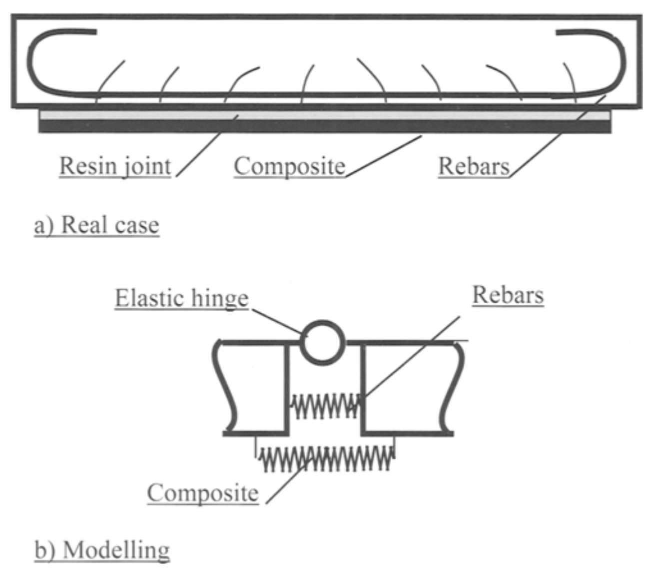

Fig. 4 - Modelling of a cracked RC beam with composite strengthening.

[11], the evaluation of the steel rebars active length is further more complicated. Indeed, when a crack occurs, the concrete envelope is damaged (yielding and failure) in the crack vicinity and the steel rebars are involved. As a consequence, the steel rebars active length depends on the elastic force transfer along the rebars and of the concrete envelope damaging in the vicinity of cracks. It is worth noting that the excitation level is low enough to prevent a steel-concrete slipping that can be considered as damage. Such an assumption is in agreement with the purpose of a non-destructive assessment of the dynamic characteristics of the beam. The steel rebars active length L_{steel} is evaluated from experimental results when the beam features a 10 kN cracking pattern (Table 2): this parameter is determined by inverse analysis equalling the first natural frequency obtained from the modelling, with the

measured value. A 20 mm long steel rebars active length L_{steel} is then identified. Table 2 clearly shows that the strengthening of the cracked section due to the rebars must be taken into account in the modelling.

The longitudinal stiffness k_{steel} of the rebars (Young's modulus E_{steel}, cross section S_{steel}) along their active length L_{steel} is given by:

$$k_{steel} = \frac{E_{steel}\, S_{steel}}{L_{steel}} \tag{12}$$

Then the rotation stiffness associated with the rebars k^{θ}_{steel} is:

$$k^{\theta}_{steel} = h^2\, k_{steel} \tag{13}$$

The cracked RC section with an external strengthening is modelled by an elastic hinge whose stiffness k^{θ}_{hinge} is given by:

$$k^{\theta}_{hinge} = k^{\theta}_{crack} + k^{\theta}_{steel} + k^{\theta}_{repair} \tag{14}$$

The resulting stiffness of the elastic hinge is used in Equation (5) and then in Equation (2) to compute the frequencies. Note that L_{steel} in Equation (12) is the governing parameter.

4.2 Experimental validation

The five first bending frequencies of a small scale model with a 10 kN cracking pattern are measured with free-free boundary conditions when the beam is unloaded (Table 2). Then, the composite strengthening is applied on the tensile face of the beam and its first natural frequencies are measured (Table 3). Experimental data are compared to the analytical ones.

The error is lower than 6% on all the five first modes. Then, such a modelling is considered for the prediction of the first bending frequencies of a cracked RC beam with composite reinforcement.

Table 3 - Natural frequencies (Hz) of a cracked RC beam (10 kN) with composite

Mode number	Experiment (Hz)	Modelling (Hz)	Difference (%)
1	455	466	2.4
2	1189	1239	4.2
3	2179	2316	6.3
4	3274	3459	5.6
5	4588	4840	5.5

5. DAMAGE ASSESSMENT OF A CRACKED RC BEAM

The natural frequencies of a structure vary when this latter is damaged. So, if the relation between the damage level and the natural frequencies variation is known, it is possible to assess the damage of a structure by measuring the natural frequencies. Obviously, the difficulty is to determine this relation a priori. Indeed, this involves knowing the location, the length and the number of the cracks for a given load Q, to evaluate the parameters of the model described above. Thanks to the standard codes (such as BAEL, Eurocode), a cracking pattern prevision may be proposed and then, it is implemented as an input of the analytical modelling to compute the evolution of the natural frequencies of a beam which was submitted to a static loading.

5.1 Assumptions

The prevision of the natural frequencies of the beam considers the following assumptions:

- The cracks are in a permanent open state caused by a static loading.
- The assessment of the structural data is non-destructive. The excitation level provided is low enough so as to prevent non-linear effects such as crack breathing and concrete-rebars interface slipping.

5.2 Cracking pattern prevision

5.2.1 The crack location

The cracking pattern prevision is based on the evaluation of the curvature and of the neutral axis position at the sections where a crack can occur. This prediction is done with respect to the assumptions of the BAEL code concerning the elastic field of a cracked beam [5]. First, for a given load Q, a bending moment diagram is calculated and the cracked zone is defined (Fig. 5). It corresponds to the zone where the value of the bending moment exceeds the cracking moment M_{cr}.

The cracked zone starts at an axial coordinate x_{cr} given by:

$$x_{cr} = \frac{2M_{cr}}{Q} \tag{15}$$

M_{cr} is the cracking moment:

$$M_{cr} = \frac{I_0\, f_{tj}}{0.5\, h} \tag{16}$$

where:

- f_{tj} is the concrete tension strength,
- h is the beam height,
- I_o is the inertia of an uncracked section.

The maximum value of the bending moment is reached inside the pure flexion zone. Inside this zone, the cracks start out vertically with a spacing quoted ΔL in Fig. 5. ΔL is evaluated from the minimal crack spacing ΔL_{min} that depends on the rebar-to-concrete bond strength τ_d.

ΔL_{min} is given by:

$$\Delta L_{\min} = \frac{B\, f_{tj}}{\tau_d\, \pi\, d_S} \tag{17}$$

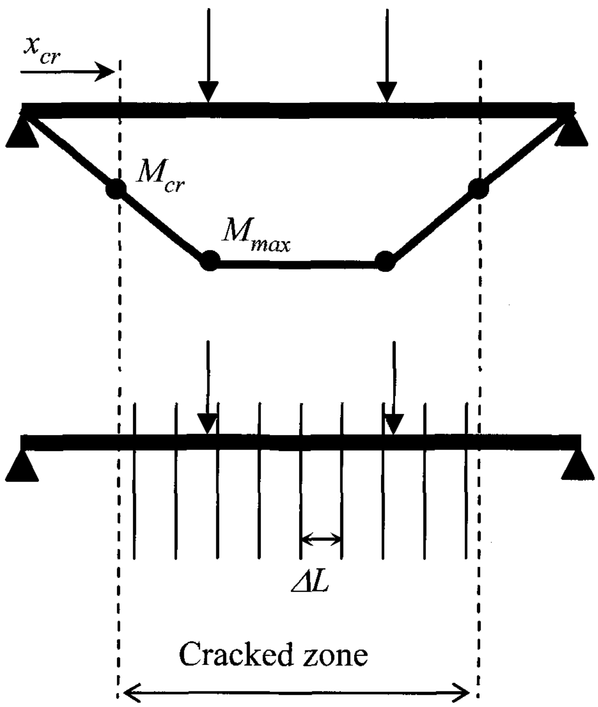

Fig. 5 - Bending moment diagram and crack locations.

where:

- B is the intact beam cross section,
- d_S is the steel rebars diameter,
- the bond strength τ_d is given by:

$$\tau_d = \psi^2 f_{tj} \tag{18}$$

and ψ= 1.5 and 1 for ribbed and smooth rebars respectively.

Considering the tension transfer along the rebars, the cracks can either be spaced by ΔL_{min} or $2\Delta L_{min}$. Then, BAEL code defines crack spacing ΔL as:

$$\Delta L = 1.8\Delta L_{\min} \tag{19}$$

For the reference beam, Equations (18) and (19) lead to approximately 300 mm crack spacing, which is in concordance with experiments. Empiric factors are only available for real size concrete beams. However, crack spacing can be computed for the small-scale model using the geometric scale factor (1/3). Applying this factor to the 1:1 scale crack spacing gives an approximately 100 mm crack spacing on the scale models which is comparable to the experimentally observed one (85 mm).

5.2.2 Crack length

The curvature along the span is deduced from the bending moment diagram (Fig. 6). From one tip to the limit of the cracked zone, the curvature increases linearly from 0 up to Φ_0. Then, from the beginning of the cracked zone up to the pure flexural zone, the curvature increases linearly from Φ_0 to Φ_{max}. The extreme value of the curvature is given by:

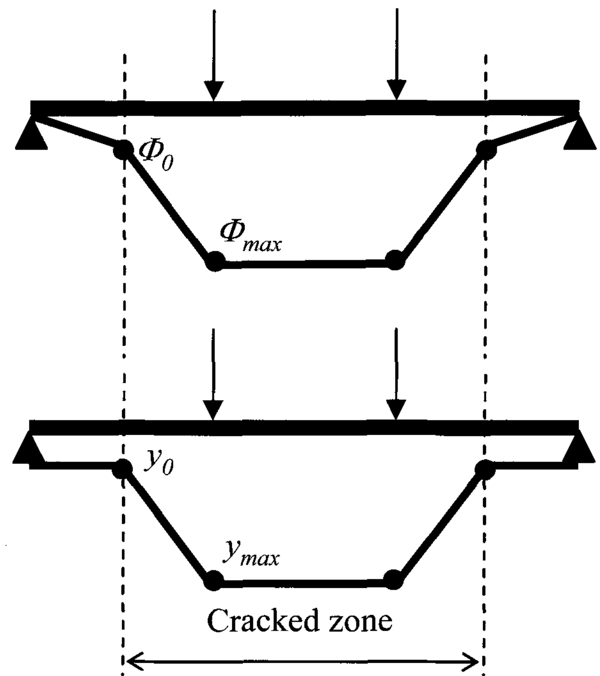

Fig. 6 - Curvature diagram and neutral axis position diagram.

$$\Phi_{\max} = \frac{\varepsilon_{s\max}}{d - y_{\max}} \tag{20}$$

where y_{max} is the extreme position of the neutral axis. ε_s and $\varepsilon_{s\,max}$ are respectively the strain and the extreme strain of the tension rebars (Fig. 7). $\varepsilon_{s\,max}$ is given by:

$$\varepsilon_{s\max} = \frac{M_{\max}}{E_{steel}\, S_{steel}\,(d - y_{\max})} \tag{21}$$

The neutral axis position is also deduced from the bending moment diagram (Fig. 6). In the uncracked zone ($x<x_{cr}$), the neutral axis position (y_0) is given by the centroid of the homogenized section. In the pure flexural zone, the neutral axis position is fixed to y_{max}, which is given by:

$$y_{\max} = 0.3d \tag{22}$$

From the beginning of the cracked zone up to the pure flexural zone, the neutral axis increases linearly.

Once the curvature and the neutral axis diagrams are calculated, a strain diagram is established (Fig. 7). The crack length a is calculated considering that the crack tip corresponds to the point of the diagram where the tension strength of the concrete is matched. The strain at this point is ε_{lim} and is given by:

$$\varepsilon_{\lim} = \frac{f_{tj}}{E_{concrete}} \tag{23}$$

Then the crack length a is given by:

$$\Phi = \frac{\varepsilon_{\lim}}{h - y - a} \tag{24}$$

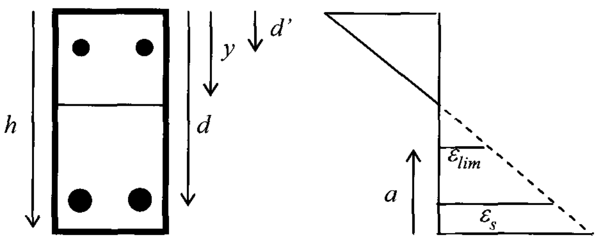

Fig. 7 - Strain diagram at a cracked section.

5.3 The natural frequencies evolution and the damage structure level

A four-point bending test is carried out on a small-scale model. For various values of the bending moment M, the cracking pattern is measured (crack location and crack length) and the beam is unloaded and placed in free-free boundary conditions so as to measure its natural frequencies associated with the five first bending modes $f_i(M)$. Then, for each static loading level, the relative variations $\Delta f_i(M)$ are calculated:

$$\Delta f_i(M) = 100 \cdot \frac{f_i(0) - f_i(M)}{f_i(M)} \tag{25}$$

These experimental data are compared to the analytical ones obtained for both following cases:

1. The measured cracking pattern is used as an input of the model.
2. The predicted cracking pattern described above is used as an input of the model.

The results clearly show that the natural frequencies decrease when the bending moment increases (Figs. 8 and 9). Two plateaus are observed. The first one appears when the cracking moment is reached. Then, three cracks start out in the flexural zone. When the bending moment increases and matches 0.3 kNm, the cracking pattern is extended to the flexural-shear zone where new cracks start out, resulting in the second plateau. The curves for the five first experimental natural frequencies are similar to the analytical curves obtained when the experimental cracking pattern is taken into account (Figs. 8 and 9): more particularly, the two plateaus are clearly observed as well as the abrupt transition between them. The difference does not exceed 20% for the two first modes. When the prediction is used, the results are in agreement with those obtained when the crack length is measured.

For the higher frequencies, the difference between experiments and modelling increases with the number of the mode, even if the two plateaus are correctly described. These differences can be explained by:

- The use of beam element for the modelling despite

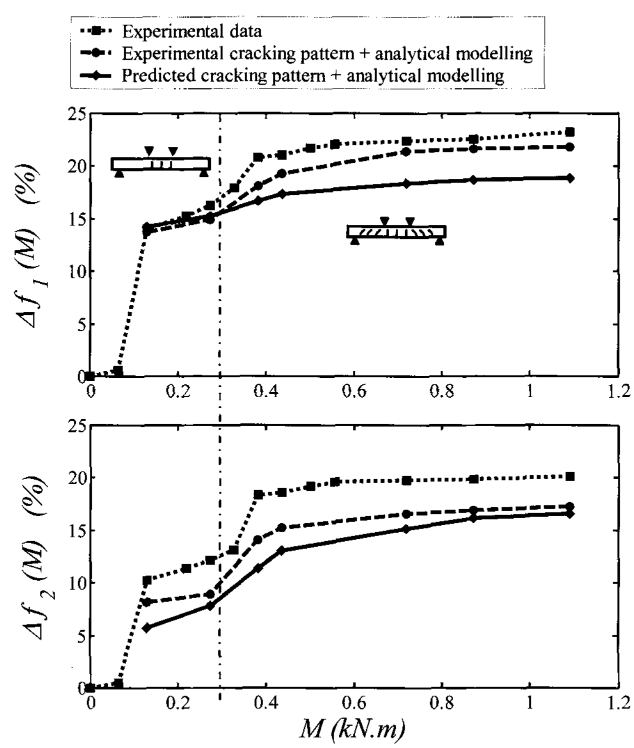

Fig. 8 - Relative variation of frequencies for the two first bending modes.

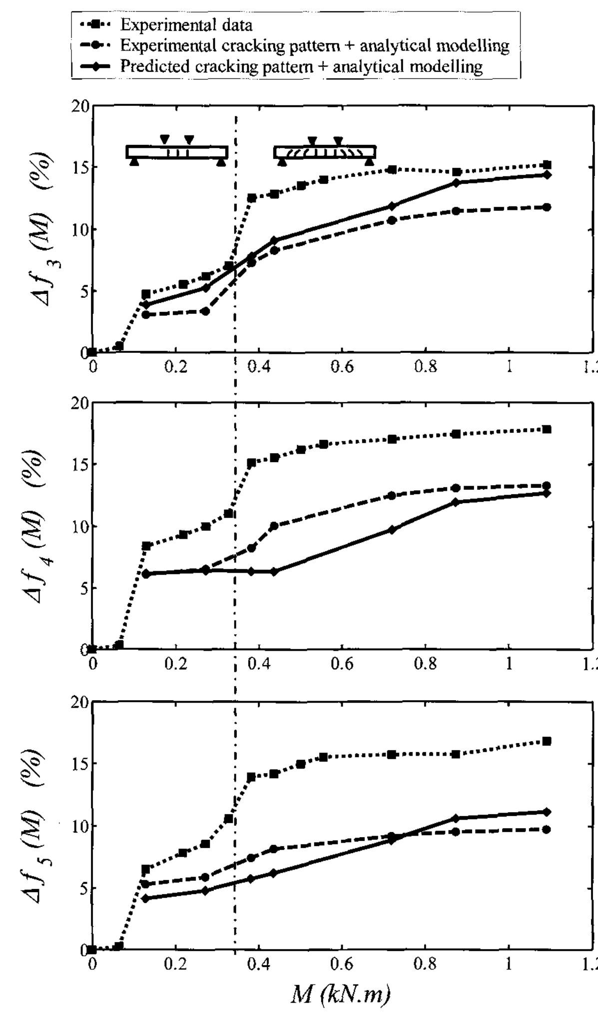

Fig. 9 - Relative variation of frequencies for the third, fourth and fifth bending modes.

small crack spacing: a three-dimensional modelling would be better.

- The actual opening modes of the flexural-shear cracks are more complex than the predicted cracking pattern used: for instance, nonlinearities are probably involved and, are not taken into account.
- The cracks are supposed to be vertical, that is not true for the flexural-shear ones: that has an influence on the crack length. This is why the analytical modeling, associated with the experimental cracking pattern provides some better results.

These points are to be taken into account for more accuracy of the modelling concerning the higher modes. Nevertheless, it is worth noting that only the very first modes are generally taken into account for the dynamic response evaluation of civil engineering structures.

5.4 Discussion

The aim of this discussion is to explain why two plateaus are observed. The first plateau occurs with the flexural cracks. The second plateau occurs with flexural-shear cracks. During the test, the length of these cracks increases. Then, the plateaus reveal that the frequencies are not greatly influenced by the crack growth. This can be explained by considering the parameter η_{steel}:

$$\eta_{steel} = 100 \cdot \frac{k^{\theta}_{steel}}{k^{\theta}_{hinge}} \tag{26}$$

This parameter characterizes the relative contribution of the rebar stiffness to the stiffness of a cracked section that is modelled by its equivalent elastic hinge Equation (14).

The contribution η_{steel} is plotted as a function of the ratio of the crack length under the beam height Fig. 10. It clearly shows that η_{steel} increases with crack length. When the crack length is half the beam height, steel reinforcement accounts for 80% of the entire stiffness of the cracked section: when crack length increases the stiffness of the cracked section stabilizes with the predominant rebars stiffness. As a consequence, in a first approximation, the cracked sections can be modelled by considering entirely cracked sections. Only the number and the location of the cracks can be considered.

6. CONCLUSION AND OUTLOOKS

This work should be viewed as a first-order attempt at a damage assessment of a RC-beam (with or without strengthening) by a natural frequency measurement.

This is based on an analytical model developed in [10] and modified to be applied to a crack reinforced concrete beam.

In a first step, the influence of the steel reinforcement on the natural frequencies of a cracked beam has been studied. It appeared that the steel reinforcement is characterized by:

- A non-significant influence when the beam is not cracked. The beam can then be modelled as a homogeneous one.

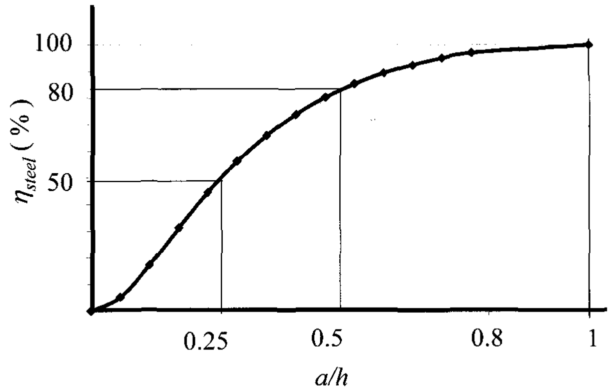

Fig. 10 - Steel rebars contribution to the stiffness of a cracked section.

- A significant influence when the beam is cracked. The rebars act as crack bridging elements.

As a first conclusion, the rebars can be modelled in the same manner as a composite external strengthening. So, the cracked beam is modelled by an assembly of beam elements with elastic hinges. The stiffness of the hinges takes into account the flexibilities associated with the cracks and the stiffness of the bridging effects of both the composite and the rebars strengthening. The stiffness induced by the rebars depends on the active length of the rebars: this parameter is obtained so as the first modelling natural frequency corresponds to the first experimental one. The model of a cracked RC beam with a composite strengthening is experimentally validated on a small-scale model.

In a second step, the analytical model is used as a damage assessment tool. A prevision of a simplified cracking pattern with vertical cracks is needed. It is based on the determination of the curvature and of the neutral axis position at the sections where a crack can appear. This prevision is implemented as an input of the analytical model so as to provide the frequencies as a function of the static loading. A small-scale model has been used for the validation of this approach. The two plateaus that can be observed by plotting the evolution of the frequencies with respect to the bending moment are due to the important contribution of steel rebars to the stiffness of the cracked sections.

The natural frequencies measurements presented in this paper are carried out with free-free boundary conditions. Hence no variations between two distinct measurements are introduced, which is less true with some other boundary conditions. The experimental data base obtained is then more adequate for model validation. However the approach is general and can be apply with any boundary conditions. Therefore it can be implemented on a real structure with clamped or simply supported boundary conditions. So, with the modelling, it is possible to determine a priori some curves such as the ones represented in Figs. 8 and 9. Then, to assess the structure damage, the following procedure may be followed:

1. A frequency measurement of the first natural frequencies of the intact structure.

2. A frequency measurement of the first natural frequencies of the structure when a damage assessment is required.
3. With the curves such as the ones represented in Figs. 8 and 9, we can read the maximal moment applied to the structure: this is the abscissa of the point of which the ordinate is the natural frequency shift.

The knowledge of this moment allows then to deduce a damage assessment by comparison with the cracking moment.

The accuracy for the prediction of the frequencies for higher modes can be ameliorated. This will be undertaken by:

- Using short beam element models.
- Describing better the complex flexural-shear cracks.

Furthermore, higher excitation levels may be considered to identify the non-linear effects that can be activated (crack breathing, slipping of the concrete-rebars interface). Such an analytical approach would be useful for the determination of the dynamic response of structures consisting of a cracked concrete substructure assembly. This structure could either be subject to a composite external strengthening or not. The application field would no longer be a structure monitoring but would be dedicated to the seismic behaviour prediction.

REFERENCES

[1] Ferrier, E. and Hamelin P., 'Long time concrete composite interface characterization for reliability prediction of RC beam strengthened with FRP', *Mater. Struct.* **35** (253) 564-572.

[2] Bizindavyi, L. and Neale, K.W., 'Transfer lengths and bond strength for composites bonded to concrete', *Journal of Composites for Construction* **3** (4) (1999) 153-160.

[3] Chajes, M.J. and Finch, W.W.Jr., 'Bond and force transfer of composite material plates bonded to concrete', *ACI structural Journal* **93** (2) (1996) 208-217.

[4] Meier, U., Deuring, M., Meier, H. and Schwegler, G., 'Strengthening of structures with CFRP laminates: research and applications in Switzerland', in Proceedings of ACMBS'1 Canada, 1992 243-251.

[5] Triantafillou, T., 'Shear strengthening of reinforced concrete beams using epoxy-bonded FRP', *Composites ACI Structural Journal* **95** (2) (1998) 107-115.

[6] Ovigne, P.-A., Massenzio, M., Jacquelin, E. and Hamelin, P., 'Analytical model for the prediction of the eigen modes of a beam with open cracks and external strengthening', *Structural Engineering and Mechanics* **15** (4) (2003) 437-449.

[7] Ovigne, P.-A., Massenzio, M., Jacquelin, E. and Hamelin, P., 'Crack bridging force transfer of composite strengthening: a dynamic point of view', *Steel and Composite Structures* **3** (1) (2003) 33-46.

[8] Jerath, S. and Shibani, M.M., 'Dynamic stiffness and vibration of reinforced concrete beams', *ACI Journal* **82** (2) (1985).

[9] Johns, K.C. and Belanger, M.D., 'Dynamic stiffness of concrete beams', *ACI Journal* **78** (3) (1981).

[10] Wang, Z., Man, X.-T.C., Finch, R.D. and Jansen, B.H., 'The dynamic behavior and vibration monitoring of reinforced concrete beams', *J. of Testing and Evaluation* **26** (5) (1998) 405-419.

[11] Dreux, G., 'Calcul pratique du béton armé - Règles BAEL 83' (Eyrolles, Paris, 1988).

[12] Varastehpour, H., 'Optimisation du renforcement des ouvrages en béton armé par des matériaux composites', Thesis, University Lyon 1, France, 1996, 214 p.

[13] Gudmundson, P., 'The dynamic behavior of slender structures with cross sectional cracks', *J. Mech. Phy. Sol.* **31** (4) (1983) 329-345.

[14] Papadopoulos, C.A. and Dimarogonas, A.D., 'Coupled longitudinal and bending vibrations of a rotating shaft with an open crack', *J. Sound and Vibration* **117** (1) (1987) 81-93.

[15] Täljsten, B., 'Defining anchor lengths of steel and CFRP plates bonded to concrete', *Int. J. of Adhesives* **17** (4) (1997).

[16] Täljsten, B., 'Strengthening of beams by plate bonding', *J. of Materials in Civil Engineering* **9** (4) (1997) 206-212.

[17] Fuentes, A., 'Le béton armé après fissuration' (Eyrolles, Paris, 1980).